Environ Sci Pollut Res (2016) 23:16722–16737
DOI 10.1007/s11356-016-6834-7

RESEARCH ARTICLE

Water-soluble ionic species of coarse and fine particulate matter and gas precursor characteristics at urban and rural sites of central Taiwan

Jiun-Horng Tsai[1] · **Su-Mei Tsai**[2] · **Wei-Chi Wang**[3] · **Hung-Lung Chiang**[3]

Received: 19 June 2015 / Accepted: 4 May 2016 / Published online: 17 May 2016

Abstract Coarse and fine particulate matter (PM) were taken by a dichotomous sampler, and gas precursors were determined by a denuder sampler at two stations in central Taiwan. Water-soluble ionic constituents of PM and their precursor gases were analyzed by ionic chromatograph. In summer, the daytime/nighttime PM_{10} concentrations were 37 ± 10/41 ± 18 μg m^{-3} and 36 ± 14/34 ± 18 μg m^{-3} for Xitun and Jhushan, respectively. Average PM_{10} concentration in winter was 1.55 and 1.76 times that of summer for Xitun and Jhushan, respectively. PM mass concentrations were similar for both stations, although one station is located in the downtown area of Taichung, and the other is in a rural area with no heavy pollution sources. Water-soluble ionic species content was 38–53 % of $PM_{2.5}$ and 43–48 % of PM_{10} mass concentration. HNO_3, HCl, and SO_2 were high in the daytime; the daytime-to-nighttime concentration ratio was 3.75–6.88 for HNO_3,1.7–7.8 for HCl, and 1.45–2.77 for SO_2. High NH_3 levels were determined in the area, especially in winter, which could be a precursor of NH_4^+ to form particulate matter. In Xitun, motor vehicles downtown and in the industrial district could be sources of air pollution. In contrast, there are few industrial sources at Jhushan; therefore, the transport of air pollutants from upwind of other regions and the accumulation of pollutants could be important PM sources at Jhushan.

Keywords $PM_{2.5}$ · $PM_{2.5–10}$ · Water-soluble ionic species · Gas precursor

Responsible editor: Philippe Garrigues

✉ Hung-Lung Chiang
hlchiang@mail.cmu.edu.tw

[1] Department of Environmental Engineering, Sustainable Environmental Research Center, National Cheng-Kung University, Tainan, Taiwan

[2] Department of Landscape Architecture, Tunghai University, Taichung, Taiwan

[3] Department of Health Risk Management, China Medical University, Taichung 40402, Taiwan

Introduction

Particulate matter (PM) is an important indicator of air pollution emitted from a variety of natural and anthropogenic activities. PM can be suspended a long time and travel long distances in the atmosphere, and it can cause a wide range of diseases and lead to a significant reduction of human life (Kim et al. 2015). PM pollution has aroused worldwide concerns due to its significant adverse effects on visibility, public health, and even global climate (Okada et al. 2001; Kang et al. 2004; Sun et al. 2006, 2014; Tan et al. 2009).

According to the mass fraction of ionic species, SO_4^{2-}, NH_4^+, and K^+ were predominant in fine particulate matter. Nitrate existed in both the fine and coarse particulate matter due to the different formation mechanisms. In addition, SO_4^{2-} and NH_4^+ were foremost in fine particles (Wall et al. 1988). Na^+, Ca^{2+}, and Mg^{2+} predominated in the coarse particulate matter, and the erosion of soil, crustal rock, and sea salt spray could be the sources of these ions.

$PM_{2.5}$ can go deeper into the nonciliated and alveolar areas of the lungs; therefore, $PM_{2.5}$ has been reported to have greater health effects than larger particulate matter from inhalation exposure causing allergies, asthma, and cardiovascular disease (Spengler et al. 1990; Glodberg et al. 2001; Hoek et al. 2002; Gauvin et al. 2002; Jalaludin et al. 2004; Kappos et al. 2004; Breysse et al. 2013; Conti et al. 2015; Kim et al. 2015). Based on estimates by Cohen et al. (2005), $PM_{2.5}$ ambient air pollution is responsible for approximately 0.8 million

premature deaths and 6.4 million years of life lost worldwide every year.

Sulfate, nitrate, and ammonium were the dominant components of water-soluble ions in PM, except for organic species (Aneja et al. 2006; Hsieh et al. 2009; Lin et al. 2009; Plaza et al. 2011; Wang et al. 2014). Up to 80 % of nitrate and ammonium in fine particles was formed from precursor gases and mobile sources including diesel engines and gasoline engines in the South Coast Air Basin (Ying and Kleeman 2006). In an industrial and urban city of Korea, ionic constituents accounted for 35–60 % of $PM_{2.5}$mass, and sulfate and nitrate were the major ionic species (Han et al. 2008). Plaza et al. (2011) indicated that the sulfate and ammonium mass was concentrated in the fine mode, and nitrate concentration was high in the coarse mode in an urban area of Madrid. The gas phase and condensation processes for secondary aerosol formation could be important mechanisms in the urban area of Madrid. NH_4^+, SO_4^{2-}, NO_3^-, and Cl^- were the major water-soluble inorganic ionic constituents of $PM_{2.5}$, and NH_3, HNO_3, and HCl were the important precursor gases (Sudheer and Rengarajan 2015). Therefore, sulfate, nitrate, and ammonium are the important constituents in fine particles, and SO_2, NOx, and NH_3 could be their gas precursors.

Many previous studies have indicated that ammonia is an important precursor in the formation of fine particles in the USA (Heald et al. 2012; Benedict et al. 2013; Gong et al. 2013; Li et al. 2014), Europe (Minguillón et al. 2012; Reche et al. 2012), Japan (Sakurai and Fujita 2002; Aikawa et al. 2013), Korea (Phan et al. 2013), India (Behera and Sharma 2010; Sudheer and Rengarajan 2015), China (Hu et al. 2008; Shen et al. 2011), and Taiwan (Tsai et al. 2014). NH_3 is considered to be a potentially important participant in aerosol nucleation and formation (Kirkby et al. 2011), and it can easily transfer into the particulate phase as NH_4^+ through reaction in the atmosphere (Walker et al. 2004; Plessow et al. 2005). Therefore, gas precursors converging to form an aerosol could be important sources of fine particulate matter.

In this study, the coarse and fine particulate matters were collected by a dichotomous sampler, and gas precursors were determined by a denuder sampler. Water-soluble ionic species for particulate constituents and gaseous pollutants were measured during the day and night in summer and winter. In addition, the effects of meteorological parameters and precursor gases on the characteristics of particulate matter were explained.

Experimental

Sampling location

Two stations of the Taiwan Air Quality Monitoring Network (which was established by the Taiwan Environmental Protection Agency [TEPA] in 1993), Xitun (Taichung) and Jhushan (Nantou), were chosen as sampling sites for the experiment (Fig. 1). Xitun station is located in Taichung City, and Jhushan station is located in Nantou County. Xitun is in the downtown area and near industrial districts, but Jhushan is

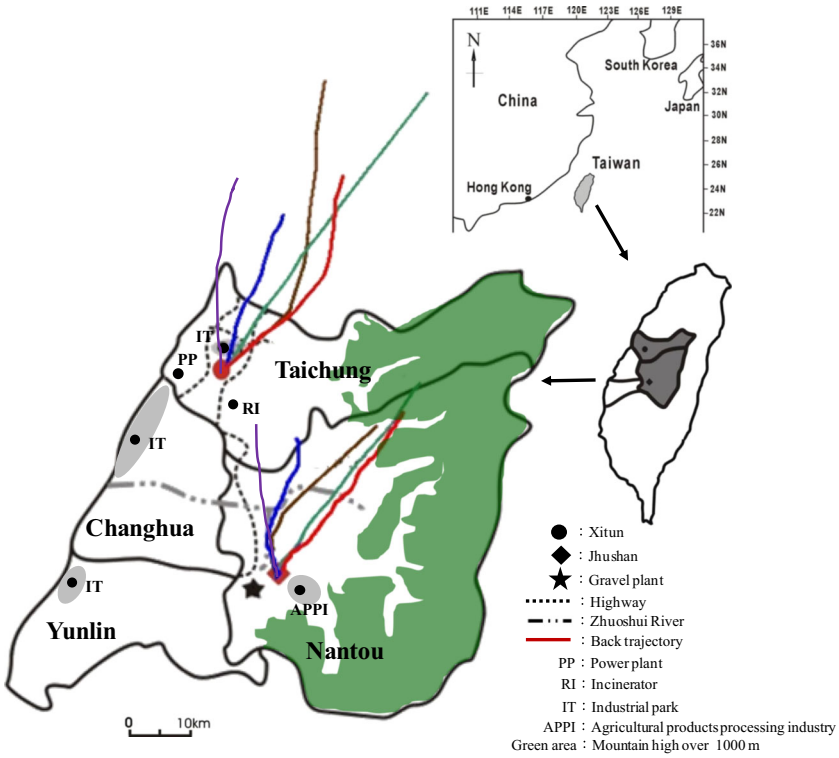

Fig. 1 Map of emission sources in the vicinity of sampling sites in central Taiwan

a rural area, and heavy transportation loading could be the source of air pollutants. Taichung is the third largest city in Taiwan (Taichung County and Taichung City were merged as Taichung City on 25 December 2010), with an area of about 2, 214 km^2 and a metropolitan population of 2.69 million in 2013. The downtown population density is more than 20, 000 people km^{-2}.

Xitun is 0.3 km to the northwest of the Taichung industrial district, the municipal waste incinerator is 2.6 km to the southwest, and Central Taiwan Science Park is 4 km to the northeast. The coastline is 14 km to the west. Freeway 1 is 0.3 km to the east, freeway 3 is 6 km to the west, and highway 74 is 1 km to the east.

In downtown Taichung, pollution emissions were 5, 900 tons $year^{-1}$ for PM_{10}, 2,400 tons $year^{-1}$ for $PM_{2.5}$, 660 tons $year^{-1}$ for SO_2, 11,200 tons $year^{-1}$ for NOx, and 26,700 tons $year^{-1}$ for NMHC. The sources of PM_{10} were 68 % from construction and road dust, 17 % from vehicles and 14 % from commercial and industrial sources. Emissions from industrial and commercial sources account for 86 % of SO_2, and vehicle emissions account for 90 % of NOx (TEPA 2015). The emission intensity was shown as Fig. 2.

Conversely, Jhushan is 48 km from the western coastline, and the major pollution sources in the region are several gravel plants (2–3 km west of the station) and the Jhushan industrial district (3 km northeast) for agricultural product facilities. In Nantou, PM_{10} was 7,500 tons $year^{-1}$, $PM_{2.5}$ was 3, 100 tons $year^{-1}$, SO_2 was 620 tons $year^{-1}$, NOx was 8, 200 tons $year^{-1}$, and NMHC was 12,400 tons $year^{-1}$. The sources of PM_{10} were 71 % from construction and road dust, 9 % from vehicles and 16 % from commercial and industrial sources. Eighty-eight percent of SO_2 was emitted from commercial and industrial sources, and 85 % of NOx was emitted from vehicles. In addition, open burning contributed 7 % of $PM_{2.5}$ emission in Nantou (TEPA 2015).

The experiment was conducted during the periods from 27 February to 5 March, 16–21 April,12–19 May, and 4–10 July, 1–6 November 2012. The colorful lines (shown as Fig. 1) show the air parcel transport pathways by back trajectory (Lin and Chang 2002) during different sampling periods. At each site, one particulate sample was taken every 12 h, from 0700 to 1900 hours one, and from 1900 to 0700 hours the next day.

Particulate matter sampling method

Dichotomous sampler

Ambient PM was taken by a dichotomous sampler (Graseby Adenson G 241, USA) equipped with an inlet of 10-μm cutpoint. PM below 10 μm aerodynamic diameter (PM_{10}) was divided into two size fractions upon entering the sampler using a virtual impactor with a 2.5-μm cutpoint. The two size fractions were classified as a coarse fraction (2.5 μm < aerodynamic diameter < 10 μm, $PM_{10–2.5}$) and a fine fraction (aerodynamic diameter <2.5 μm, $PM_{2.5}$). The total flow rate of the dichotomous sampler was 16.7 L min^{-1}. It was split into 1.67 and 15 L min^{-1} for coarse and fine flow, respectively.

PM was collected using 37-mm quartz fiber filters (Pallflex 2500 QAT-UP, 37 mm) supported by polyolefin rings. Filters were pre-treated before sampling at 900 °C for 3 h to reduce the background level of carbonaceous species and other volatile species in the filter and to reduce the artifact effect of the filter. The pre-treated filters were placed in clean polyethylene Petri dishes, which were then wrapped with Teflon tape and aluminum foil and stored in a freezer until field sampling. The weight of the filters and the collected particulate mass concentration was measured by a microbalance (Mettler Toledo, MX5) with a reading of 1 μg. The precision of the quartz filter is ±10 μg under the condition of 40 % relative humidity at 25 °C. Prior to weighing, the filters were conditioned at 25 ± 2 °C and 40 ± 5 % relative humidity for 48 h. Filter samples were stored in a refrigerator at 4 °C before chemical analysis to limit losses of volatile components. In addition, the quartz filter was preheated to reduce interference, and blank samples and other quality assurance and quality control samples were also analyzed in this study to minimize the artifact effect of the filter.

Denuder sampler

The denuder system employed in this study was composed of a cyclone with a cut-off diameter of 2.5 μm (University Research Glassware, URG, Chapel Hill Inc., USA) followed by four annular denuders (URG-2000-30EH), a filter pack, a flow controller, and a pump (USEPA 1998). Airflow was set at a constant rate of 16.7 L min^{-1}.

The first denuder was coated with 10 ml of 0.1 % (*w*/*v*) NaCl in 1:9 methanol/deionized water solutions for the absorption of HNO_3 gas (Perrino et al. 1990; USEPA 1998). The second and third denuders were coated with 10 ml 1:1 (*v*/*v*) mixtures of 2 % (*w*/*v*) Na_2CO_3 in deionized water, and 2 % (*w*/*v*) glycerol in methanol solution for the absorption of HCl, HNO_2, and SO_2 gas. The fourth was coated with 10 ml of 1 % (*w*/*v*) citric acid in methanol solution for the absorption of NH_3 gas. Three filters placed in series followed the denuders. The first Teflon filter (Pallflex, 47 mm, pore size 2 μm, USA) was set up to collect particulate matter <2.5 μm in diameter. In order to collect acid gas that evaporated from particles or that was not completely absorbed by the denuder, the next quartz filter was coated with Na_2CO_3 solution. The last quartz filter was coated with a citric acid solution and designed to collect NH_3 evaporated from the particles. After sampling, each denuder tube and filter was extracted with deionized water and analyzed by ionic chromatography. In

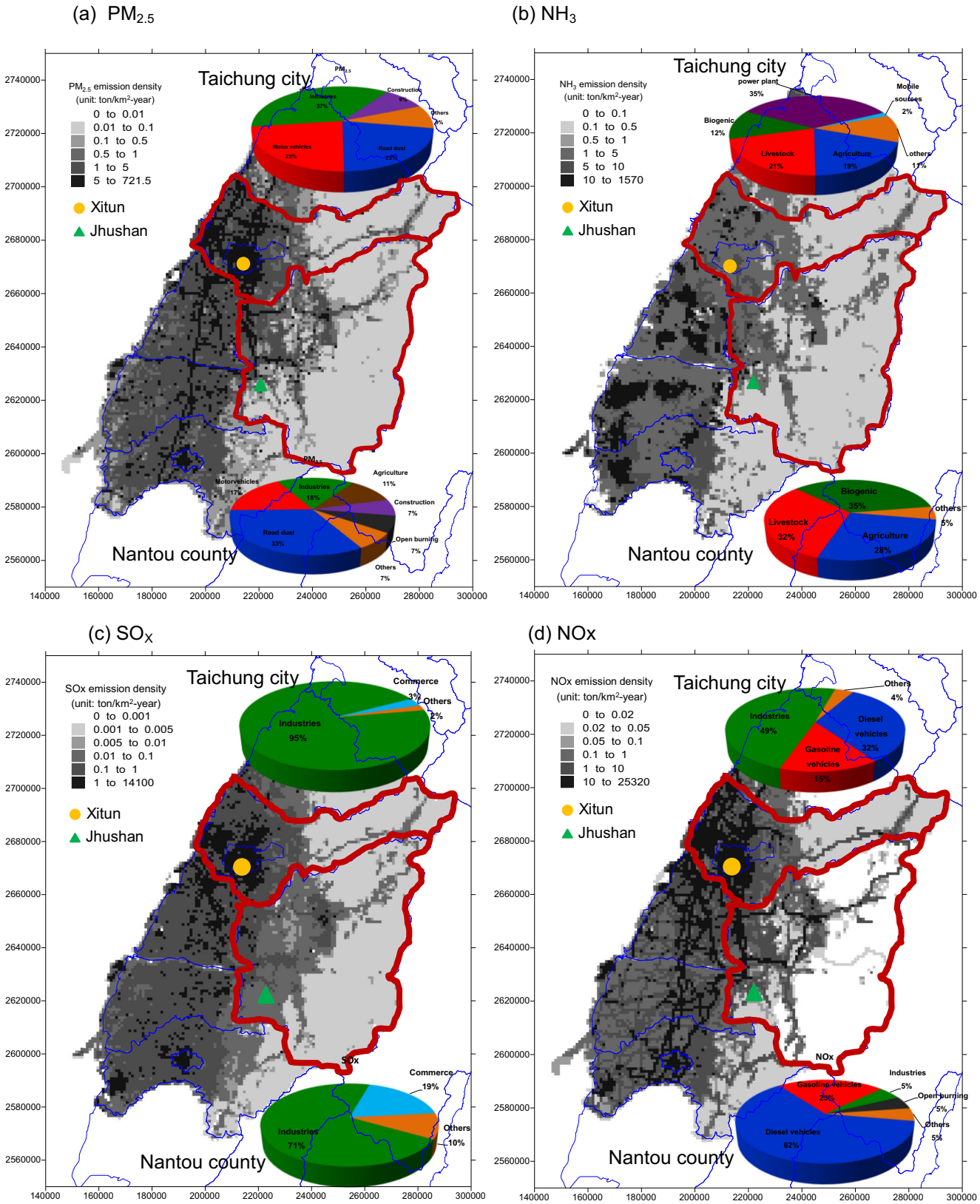

Fig. 2 Emission (ton km^{-2} yr^{-1}) (**a** $PM_{2.5}$, **b** NH_3, **c** SOx and **d** NOx) of Taiwan and source profiles of Taichung city and Nantou county at central Taiwan

addition, the additives of HNO_3, SO_2, and NH_3 gases were used to measure the recovery of the denuder adsorption system. Recoveries were 95 ± 6 % for HNO_3, 94 ± 5 % for SO_2, and 91 ± 10 % for NH_3.

Chemical analysis

The collected aerosol filters were ultrasonically extracted for 2 h into 20 ml of deionized distilled water and filtered through a Teflon filter of 0.45-μm nominal pore size. Ion chromatography (Dionex, 120) was used to analyze the concentration of anions (Br^-, F^-, Cl^-, NO_2^-, NO_3^-, SO_4^{2-}) and cations (Na^+, NH_4^+, K^+, Mg^{2+}, Ca^{2+}). The separation of anions was accomplished using an IonPac AS 12A (4 × 200 mm) analytical column, an AG 14 guard column with a 10-μl sample loop, and an anion self-regenerating suppressor-ultra. A solution of 2.7 mM Na_2CO_3/0.3 mM $NaHCO_3$ was used as an effluent at a flow rate of 1.5 ml min^{-1}. The separation of cations was accomplished using an IonPac CS 12A (4 × 250 mm) analytical column, and a CG 14 guard column, with a 50 μl sample loop, and a cation self-regenerating suppressor-ultra. A solution of 20 mM methanesulfonic acid was used as the eluent at a flow rate of 1 ml min^{-1}. Applying this analysis method, the detection limits of analyzed ionic species were in the range of 0.004 (Mg^{2+}) to 0.012 (NO_2^-) μg m^{-3}. In addition, the recoveries of ionic species were between 91 % (Na^+) and 104 % (NH_4^+).

Statistical analysis

Statistical analysis was performed by the Statistical Package for the Social Sciences (SPSS®12.0) using a student's *t* test, and differences were judged to be significant at $p < 0.05$.

Results and discussion

Particulate mass concentration

PM_{10}

The PM_{10} concentration of the dichotomous sampler consisted of $PM_{2.5}$ and $PM_{2.5–10}$. Table 1 shows the PM_{10} concentration of the dichotomous sampler. Average daytime/nighttime PM_{10} concentrations were 59 ± 13/62 ± 14 μg m^{-3} for Xitun and 59 ± 6.8/64 ± 17 μg m^{-3} for Jhushan in winter. In summer, the PM_{10} concentrations were 37 ± 10/41 ± 18 μg m^{-3} for Xitun and 36 ± 14/34 ± 18 μg m^{-3} and Jhushan. Average PM_{10} concentrations in winter were 1.55 and 1.76 times those of summer for Xitun and Jhushan, respectively. PM_{10} concentrations at night were slightly higher than during the day.

$PM_{2.5}$

Table 1 indicates the $PM_{2.5}$ concentration of the dichotomous sampler. In Xitun, the $PM_{2.5}$ concentrations were 22 ± 6.8 μg m^{-3} for daytime and 29 ± 14 μg m^{-3} for nighttime in summer. In winter, the $PM_{2.5}$ concentration increased as much as 50 % mass concentration to 34 ± 10 μg m^{-3} for daytime and 42 ± 14 μg m^{-3} for nighttime. In Jhushan, the $PM_{2.5}$ concentrations were 21 ± 7.5/21 ± 14 μg m^{-3} for daytime/nighttime in summer and 33 ± 10/42 ± 9.9 μg m^{-3} for daytime/nighttime in winter. Average $PM_{2.5}$ concentration was 50–70 % higher in winter than that in summer.

The fine particulate matter fraction was 0.55–0.59 and 0.61–71 of PM_{10} for daytime and nighttime at both stations. There was an insignificant difference of fine particulate matter fraction between seasons. But high fine particulate fraction was determined at nighttime.

Particulate matter accounts for a large portion of the air pollution in central Taiwan. But meteorological variations are also important factors influencing ambient air quality. In central Taiwan, May to September was the rainy season (summer), when pollutants are scavenged and PM is low, and the high-pollution episodes often occurred between October and February (dry season/winter) during the following year. The global solar radiation was high in summer for both stations, but the sunshine duration was similar in both seasons (Table 4). High global solar radiation and sunshine duration were determined in Xitun. Light intensity may affect the abundance of fine PM in the area for different seasons.

Table 1 Particulate matter concentrations in summer and winter

PM concentration (μg m^{-3})		Spring/summer		Winter	
		Daytime	Nighttime	Daytime	Nighttime
Xitun	$PM_{2.5–10}$	17.4 ± 4.4 (6.2–23.9)[a]	12.8 ± 4.9 (4.6–19.1)	24.9 ± 5.4 (18.2–31.3)	19.8 ± 3.8 (14.6–24.7)
	$PM_{2.5}$	21.5 ± 6.8 (8.1–33.6)	29.3 ± 14.0 (14.6–53.6)	34.4 ± 10.6 (24.0–49.4)	41.9 ± 14.5 (22.6–57.5)
	PM_{10}	36.6 ± 10.4 (17.1–49.5)	41.2 ± 17.6 (23.3–70.1)	59.3 ± 13.0 (42.6–78.2)	61.7 ± 14.4 (41.9–79.6)
Jhushan	$PM_{2.5–10}$	11.6 ± 4.0 (3.9–17)	13.7 ± 4.9 (3.6–20.5)	23.1 ± 5.3 (15.3–22.6)	18.6 ± 8.1 (8.1–20.1)
	$PM_{2.5}$	20.5 ± 7.5 (14.6–44.6)	20.8 ± 13.7 (16.8–51.6)	32.6 ± 10.0 (36–53.6)	42.0 ± 9.9 (30.1–76.4)
	PM_{10}	35.5 ± 14.0 (18.7–69)	34.2 ± 17.8 (22.4–89.7)	59.0 ± 6.8 (15.3–22.6)	64.1 ± 17.4 (44.4–89.7)

[a] Numbers in parentheses are the range of concentration

In addition, low wind speed (shown as Fig. 3) and low mixing height were determined at night, which increased PM concentrations. Emissions, subtropical weather, and topography may cause primary air pollutants to form secondary aerosols in central Taiwan.

Differences of PM mass concentration between Xitun and Jhushan stations were insignificant (p value >0.05). Generally, high emission loadings were determined in the vicinity of Xitun station, which could imply high air pollutant concentration in ambient conditions. Emissions were lower in Jhushan station, and the pollution concentration was similar to that in Xitun. The land–sea breeze could be one reason for this phenomenon. Based on the daytime and nighttime wind direction of Jhushan (Fig. 3), a land–sea breeze pattern may occur in Jhushan station. Therefore, the polluted air parcels could come from Taichung, Changhua, and Yunlin air basins associated with the sea breeze during the daytime (show as Fig. 3). But low wind speed was determined at night (shown as Table 4), so the polluted air could not be completely transported to other areas and instead accumulated in the vicinity of Jhushan, resulting PM concentrations similar to those in Xitun.

Ionic constituents

Table 2 shows the ionic species content in coarse and fine particulate matter at Xitun and Jhushan. Ionic species content ranged from 47 to 53 % for $PM_{2.5}$ and from 43 to 48 % for PM_{10} at Xitun. At Jhushan, the ionic species content ranged from 38 to 51 % for $PM_{2.5}$ and from 45 to 46 % for PM_{10}. The ionic species content fraction and mass concentration increased with the increase of PM_{10} concentration at both stations. The bulk of dry, fine-particle mass is inorganic (typically 25–75 %; Heitzenberg 1989), with NH_4^+, SO_4^{2-}, and NO_3^- as the main components. In addition, Na^+, Cl^-, Ca^{2+}, Mg^{2+}, and K^+ may be present, associated with crustal and sea-salt sources depending on the location. Results indicated that secondary water-soluble ions (SO_4^{2-}, NO_3^-, and NH_4^+) composed over 50 % of the total ions and were mainly found in fine particles. Mg^{2+} and Ca^{2+} contributed to a large fraction of the total water-soluble ions in coarse particles.

Sulfate, nitrate, ammonium, chloride, and sodium ions were the major water-soluble species in PM constituents in southern Taiwan (Lin 2002; Tsai and Chen 2006; Tsai et al. 2013, 2014). When the PM_{10} concentration was increased, the ionic species including NO_3^-, SO_4^{2-}, Cl^-, NH_4^+, Na^+, Mg^{2+}, and Ca^{2+} increased significantly (Tsai et al. 2011), which was similar to the results of this study.

For fine particles, the NO_3^-, SO_4^{2-}, and NH_4^+ increased significantly when the PM_{10} concentration went from 15 to more than 35 μg m^{-3}. In Wisconsin, USA, nitrate and sulfate concentration are influenced by regional transport and local emission to cause high $PM_{2.5}$ concentration in PM episodes (Heo et al. 2013). In addition, on-road gasoline-powered vehicles, diesel engines, natural

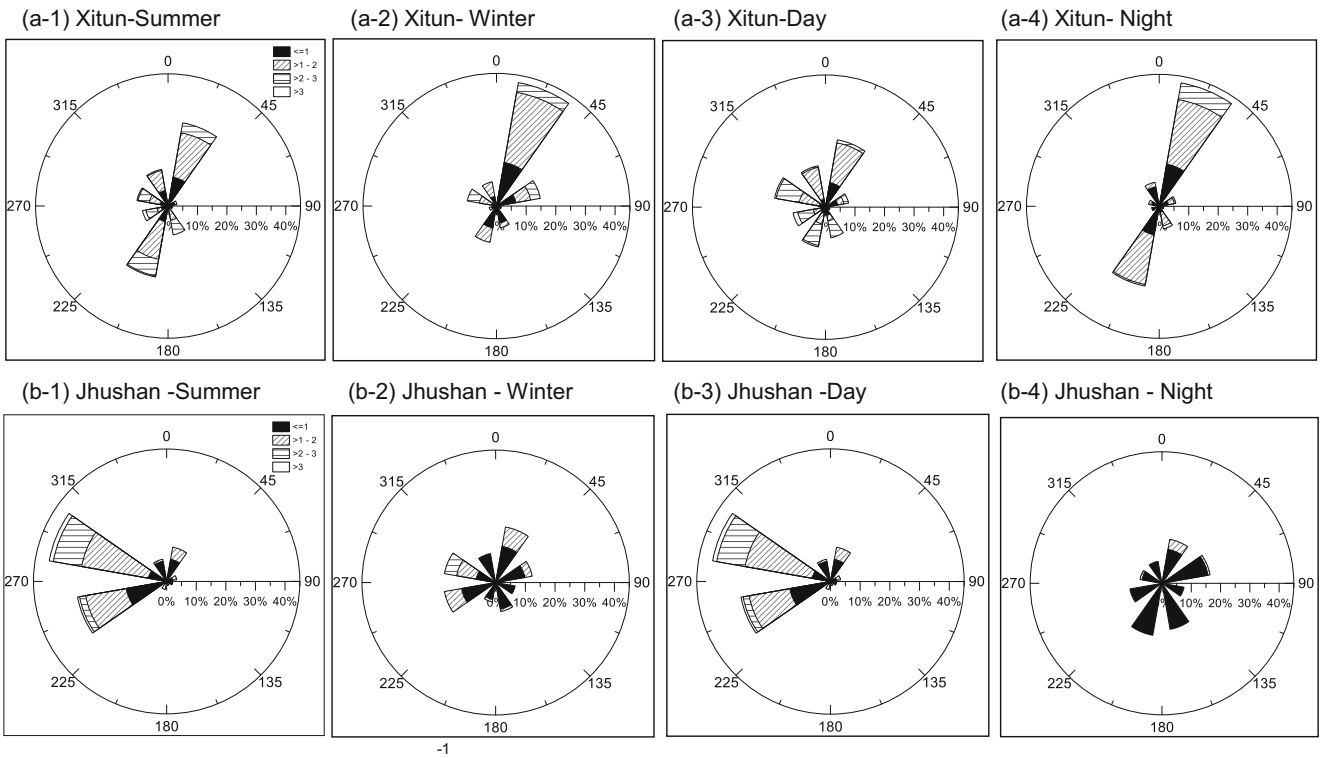

Fig. 3 Wind directions and speeds (m s^{-1}) of Xitun and Jhushan sampling sites

Table 2 Particulate mass and ionic species concentrations (in microgram per cubic meter)

Sampling site	Period	Particulate size	Concentration (μg m^{-3})	Na^+	NH_4^+	K^+	Mg^{2+}	Ca^{2+}	Cl^-	NO_2^-	NO_3^-	SO_4^{2-}	$[NH_4^+]/[SO_4^{2-}]$
Xitun	Summer	$PM_{2.5–10}$	14 ± 5.0	0.48 ± 0.44	0.35 ± 0.53	0.11 ± 0.21	0.18 ± 0.10	0.64 ± 1.04	0.68 ± 0.84	0.06 ± 0.09	1.54 ± 0.80	1.31 ± 1.40	1.42
		$PM_{2.5}$	25 ± 11	0.26 ± 0.29	2.96 ± 1.93	0.16 ± 0.09	0.14 ± 0.08	0.28 ± 0.65	0.52 ± 0.50	0.09 ± 0.11	2.85 ± 3.37	5.71 ± 3.19	2.76
	Winter	$PM_{2.5–10}$	20 ± 8.3	0.73 ± 0.46	0.15 ± 0.15	0.11 ± 0.05	0.20 ± 0.08	0.48 ± 0.26	0.59 ± 0.55	0.10 ± 0.20	3.24 ± 1.47	0.84 ± 0.69	0.95
		$PM_{2.5}$	38 ± 13	0.16 ± 0.06	5.19 ± 2.48	0.49 ± 0.30	0.16 ± 0.01	0.09 ± 0.03	0.32 ± 0.70	0.47 ± 0.64	3.41 ± 5.17	10.41 ± 3.32	2.66
	Daytime	$PM_{2.5–10}$	18 ± 6.9	0.69 ± 0.51	0.28 ± 0.56	0.08 ± 0.03	0.22 ± 0.11	0.94 ± 1.13	0.80 ± 0.94	0.08 ± 0.17	2.35 ± 1.41	1.69 ± 1.52	0.88
		$PM_{2.5}$	26 ± 10	0.32 ± 0.31	2.83 ± 1.65	0.20 ± 0.13	0.16 ± 0.08	0.38 ± 0.75	0.22 ± 0.31	0.20 ± 0.48	0.82 ± 0.82	7.39 ± 4.42	2.04
	Nighttime	$PM_{2.5–10}$	14 ± 5.6	0.48 ± 0.35	0.31 ± 0.31	0.15 ± 0.24	0.17 ± 0.07	0.26 ± 0.19	0.54 ± 0.48	0.06 ± 0.10	2.00 ± 1.19	0.69 ± 0.49	2.40
		$PM_{2.5}$	33 ± 15	0.14 ± 0.08	4.48 ± 2.26	0.33 ± 0.30	0.12 ± 0.06	0.06 ± 0.04	0.69 ± 0.67	0.22 ± 0.31	5.23 ± 4.58	6.96 ± 3.38	3.43
Jhushan	Summer, all	$PM_{2.5–10}$	7.8 ± 5.0	0.35 ± 0.28	0.40 ± 0.34	0.14 ± 0.08	0.18 ± 0.05	0.49 ± 0.72	0.31 ± 0.33	0.13 ± 0.24	1.25 ± 0.94	0.75 ± 0.92	2.84
		$PM_{2.5}$	27 ± 11	0.09 ± 0.05	2.66 ± 1.48	0.18 ± 0.07	0.15 ± 0.02	0.53 ± 0.91	0.57 ± 0.94	0.03 ± 0.06	1.50 ± 2.09	5.29 ± 2.39	2.68
	Winter, all	$PM_{2.5–10}$	15 ± 4.5	0.54 ± 0.32	0.33 ± 0.14	0.10 ± 0.02	0.19 ± 0.04	0.41 ± 0.21	0.53 ± 0.40	0.03 ± 0.09	3.84 ± 1.25	1.56 ± 2.41	1.13
		$PM_{2.5}$	46 ± 15	0.10 ± 0.03	6.41 ± 2.35	0.51 ± 0.14	0.13 ± 0.05	0.06 ± 0.02	0.15 ± 0.13	0.25 ± 0.49	5.64 ± 4.44	10.58 ± 2.47	3.23
	Daytime	$PM_{2.5–10}$	12 ± 6.3	0.52 ± 0.33	0.32 ± 0.24	0.10 ± 0.03	0.20 ± 0.05	0.57 ± 0.74	0.45 ± 0.34	0.11 ± 0.24	2.81 ± 1.79	1.53 ± 2.34	1.12
		$PM_{2.5}$	31 ± 14	0.09 ± 0.04	3.44 ± 2.14	0.30 ± 0.20	0.13 ± 0.06	0.24 ± 0.50	0.22 ± 0.45	0.17 ± 0.42	1.58 ± 2.08	6.93 ± 3.59	2.65
	Nighttime	$PM_{2.5–10}$	10 ± 5.8	0.33 ± 0.27	0.41 ± 0.30	0.14 ± 0.08	0.17 ± 0.04	0.35 ± 0.28	0.35 ± 0.40	0.07 ± 0.16	1.85 ± 1.47	0.65 ± 0.43	3.36
		$PM_{2.5}$	36 ± 20	0.09 ± 0.05	4.72 ± 3.19	0.31 ± 0.22	0.15 ± 0.02	0.40 ± 0.90	0.55 ± 0.94	0.06 ± 0.17	4.73 ± 4.57	7.49 ± 4.16	3.36

gas, and coal combustion were the major sources of nitrate, and coal combustion and natural gas were the dominant sources of sulfate in seven eastern US cities (Zhang et al. 2014).

Cao et al. (2012) indicated that sulfate, organic carbon, nitrate, and ammonium were the major constituents of $PM_{2.5}$ in Xi'an, China, and the constituents from fossil fuel combustion may have an appreciable influence on the health effects. Energy production (mainly coal combustion) was the dominant source for secondary nitrate and sulfate in Xi'an (Wang et al. 2014).

Water-soluble ions, especially for the secondary species of sulfate, nitrate, and ammonium salt, may have a surface activator to influence the heterogeneous reactions of pollutants on aerosol surfaces (Hu et al. 2008; Zhu et al. 2011). NH_4^+, SO_4^{2-}, NO_3^-, K^+, and Mg^{2+} could be in nuclei- and Aitken mode to form new particles, and NH_4^+ plays a key role in particulate formation (An et al. 2015).

Based on the molar concentration of ammonium, sulfate, and nitrate in fine particles, ammonium did not in general have a strong correlation to nitrate (r^2 was 0.52) or sulfate (r^2 was 0.49) at Xitun (Fig. 4). However, a strong correlation was found between ammonium and sulfate ($r^2 = 0.88$) and ammonium and nitrate ($r^2 = 0.81$) at Jhushan. For both stations, ammonium strongly related to the sum of equivalent molars of nitrate and sulfate.

The deliquescence relative humidity (DRH) of ammonium sulfate ($(NH_4)_2SO_4$) is 79.9 %, which is more stable than that of ammonium nitrate (DRH of NH_4NO_3 is 61.8 %) at 298 K (Seinfeld and Pandis 2006). High temperature and high humidity do not favor the formation of NH_4NO_3 in fine particulate matter. Ammonia prefers to react with sulfuric acid in the atmosphere (Baek et al. 2004), and then the excess ammonia can react with nitric acid to form NH_4NO_3 under $[NH_4^+]/[SO_4^{2-}]$ ratios higher than two. In central Taiwan, $[NH_4^+]/[SO_4^{2-}]$ ratios over two (shown as Table 2) could favor the formation of NH_4NO_3, especially in fine particles. Fine particulate nitrate is formed by homogeneous gas phase oxidation of nitrogen oxides (NOx) to gaseous nitric acid, which is followed by a reaction with gaseous ammonia to form the semi-volatile NH_4NO_3 (Ocskay et al. 2006). The distribution of NH_4NO_3 between the gas and particle phases depends mainly upon meteorological conditions (temperature and relative humidity), on the aerosol composition, and on the acidity of the particles.

The high NO_3^- at night could be due to the reaction of excess ammonium to form ammonium nitrate in fine particles and the thermal stability of NH_4NO_3 in central Taiwan. The gaseous precursors, nitric acid and ammonia, led to homogenous and heterogeneous reactions to produce NH_4NO_3 in fine particulate matter (Ravishankara 1997; Hu and Abbatt 1997; Pathak et al. 2011; Tsai et al. 2014).

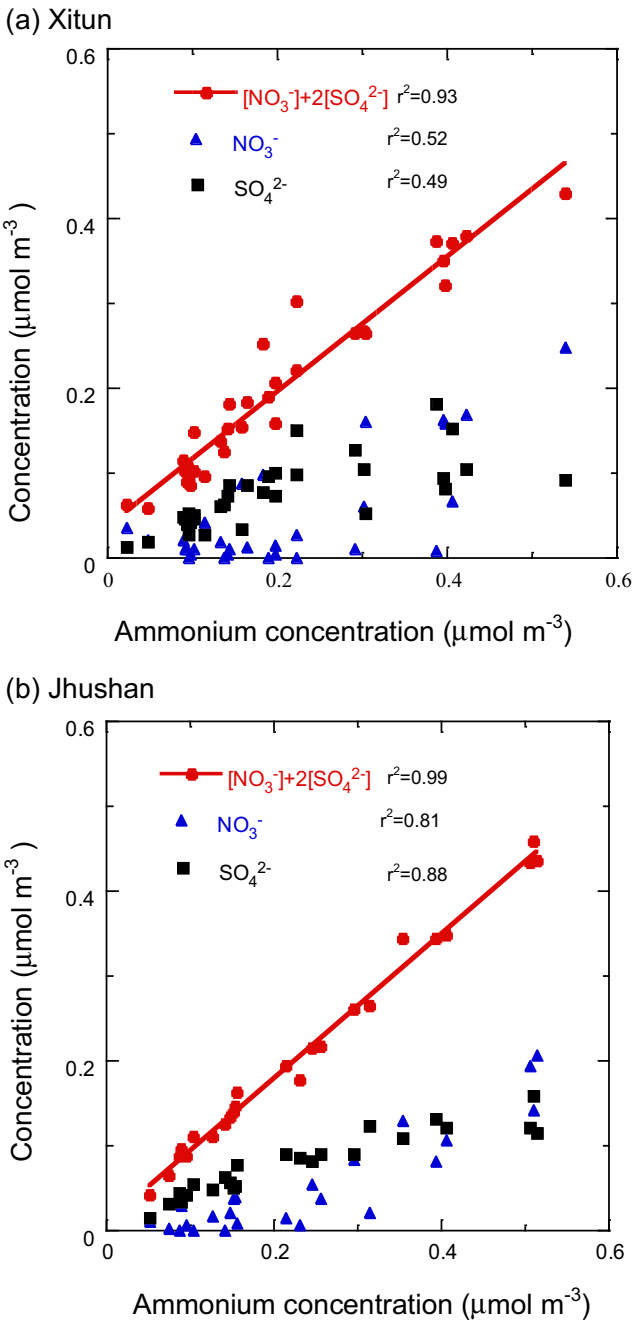

Fig. 4 Relationship of sulfate, nitrate and ammonium in fine particulate matter at **a** Xitun and **b** Jhushan

Figure 5 shows the ionic species constituents in particulate matter for different PM concentrations. Results indicated that sulfate, nitrate, and ammonium were the major ionic species in PM_{10} and $PM_{2.5}$. Three dominant ionic species increased with the increase of PM concentration. A large increase in nitrate was determined with PM_{10} concentrations over 70 μg m^{-3} for both stations. Low temperature and low humidity were determined during high PM conditions, which could enhance nitrate in PM, similar to the previous study in southern Taiwan (Tsai et al. 2014).

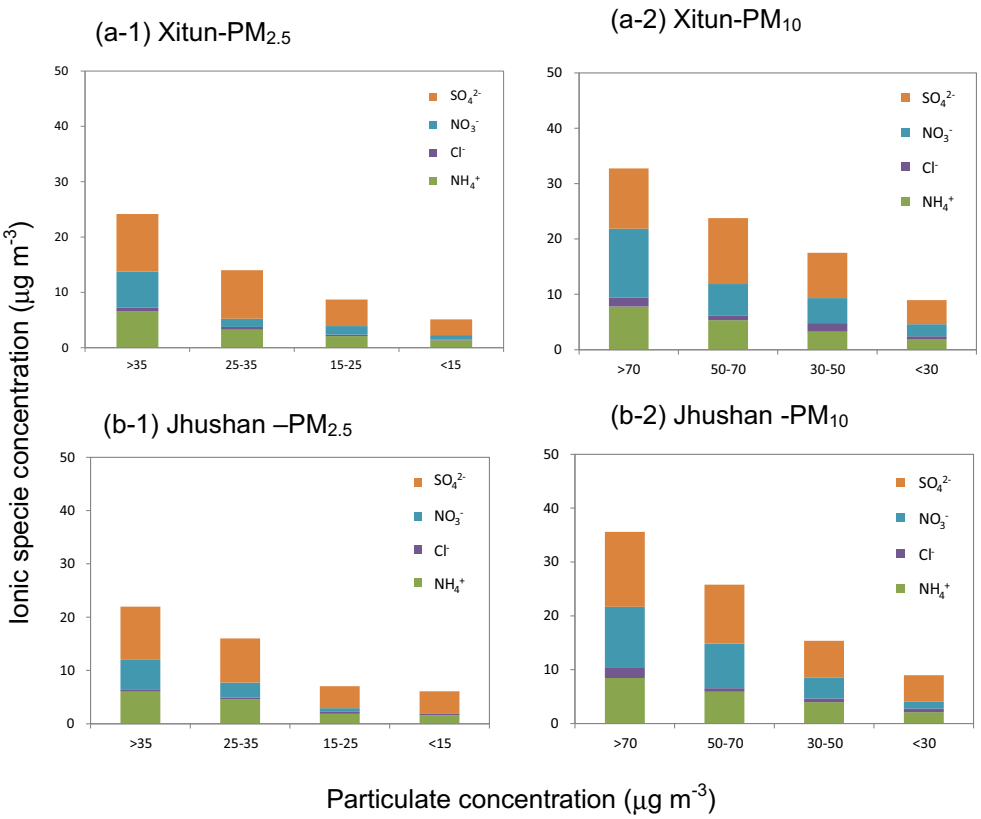

Fig. 5 Major ionic constituents at **a** Xitun and **b** Jhushan station under different PM concentrations

Gas precursors

Table 3 shows the gas precursor concentrations. High HCl concentration was determined during the day, with the average daytime concentration as much as 1.7–7.8 times higher than that at night. HCl concentrations were 4.73 and 1.86 μg m^{-3} in summer and winter, respectively, at Xitun. Similar concentrations were also determined in Jhushan.

In addition, sea-salt Cl^- depletion could increase in summer, causing elevated levels of HCl (Horemans et al. 2009). High temperatures favor the volatilization ofNH_4NO_3 and the formation of HNO_3, which in turn reacts with NaCl and results in the volatilization of Cl to form HCl (Harrison and Pio 1983; Harrison and Kito 1990; Wakamatsu et al. 1996; Pio and Lopes 1998; Vianaa et al. 2005). The reaction pathway could be the reason for the high HCl concentration in summer.

In the daytime, sea-salt particles are transported by sea breezes (wind direction shown as Fig. 3), and the reaction of NaCl with HNO_3 could release HCl in the gas phase (Thibert and Domine' 1997) to form $NaNO_3$ in coarse particles. Cl^- escapes to form HCl (Kadowaki 1977; Hitchcock et al. 1980) following the reaction of $NH_4NO_3 \rightarrow HNO_3 + NH_3$ and $HNO_3 + NaCl \rightarrow NaNO_3 + HCl$, which could contribute to the high HCl concentration in the daytime and low concentration at night.

In winter, the average HONO concentration at night (4.2 ± 2.6 μg m^{-3}) could be more than twice that observed during the day (1.8 ± 0.52 μg m^{-3}). The HONO could be removed by the photodecomposition process during the day. Nitrous acid achieves the maximum concentration at night (Calvert et al. 1994). The stronger radiation conditions are conducive to the consumption of HONO, resulting in lower HONO concentration in the daytime. The mixture of NO_2, H_2O, and NH_3 could form NH_4NO_3 aerosol and HONO gas by homogeneous nucleation, which could explain the high HONO at night (Zhang and Tao 2010).

High HNO_3 was determined in the daytime in both winter and summer. HNO_3 concentration in winter was twice that in summer. The dominant mechanism of HNO_3 could be NO_2 reacting photochemically with hydroxyl radicals after sunrise (Russell et al. 1984, 1985) to reduce the HNO_3 concentration, which could explain the high HNO_3 concentration observed during the day (Calvert and Stockwell 1983). OH radicals reacting with NO_2 could be an important reason for the higher concentration of nitric acid in the daytime. The principal mechanism of HNO_3 removal is that particulate nitrate is formed directly by reaction with NH_3 in the lower troposphere. In addition, high temperature is associated with the volatility of particulate NH_4NO_3, which could be another reason for the diurnal variation of HNO_3 concentration.

Table 3 Acid and base gases concentration (in microgram per cubic meter) in summer and winter

Gas species	Xitun				Jhushan				Taichung, Taiwan (Lin et al. 2006)	Shanghai, China (Shi et al. 2014)	Guangdong, China (Hu et al. 2008)	Ganga basin India, (Behera and Sharma 2010)	
	Summer		Winter		Summer		Winter						
	Day	Night	Day	Night	Day	Night	Day	Night				Summer	Winter
HNO_2	3.69 ± 5.81	4.00 ± 6.17	1.82 ± 0.52	4.25 ± 2.61	1.11 ± 0.75	1.42 ± 0.61	1.98 ± 0.50	4.28 ± 0.94	2.9 ± 1.4 (1.1–7.7)[a]	NA	2.9	NA	NA
HNO_3	2.51 ± 1.89	0.67 ± 1.15	4.26 ± 2.09	1.01 ± 0.16	1.79 ± 0.85	0.26 ± 0.24	3.53 ± 1.07	0.79 ± 0.39	1.9 ± 1.1 (0.4–5.3)	2.0 ± 1.8	6.3	7.6–9.9	4.8–6.5
HCl	4.73 ± 3.06	1.50 ± 1.55	1.86 ± 0.33	1.09 ± 0.53	3.98 ± 1.66	0.51 ± 0.32	2.01 ± 1.04	0.73 ± 0.21	NA	0.5 ± 0.6	2.8	NA	NA
NH_3	4.47 ± 2.30	5.64 ± 3.22	14.6 ± 6.59	20.8 ± 4.46	4.46 ± 1.61	3.62 ± 2.42	14.5 ± 5.68	17.9 ± 6.48	8.5 ± 3.0 (2.1–14.4)	6.6 ± 5.8	7.3	18.0–28.7	16.3–26.4
SO_2	7.46 ± 10.45	4.30 ± 4.13	7.72 ± 3.25	5.30 ± 4.18	3.02 ± 1.26	1.09 ± 0.96	6.97 ± 2.31	3.14 ± 1.56	NA	NA	55.4	6.8–33.3	10.5–38.2

NA not available

[a] Parenthesis presents the range of concentration

SO_2 revealed high concentration during the daytime, and the concentration difference between summer and winter was insignificant at Xitun. But at Jhushan, the SO_2 concentration in winter was as much as twice that of the concentration at summer.

Ammonia concentration was three times higher in winter than in summer for both stations. The night-time concentration of ammonia was over 30 % higher than that during the day at Xitun. In Taiwan, the ammonia emission was 206, 179 ton $year^{-1}$ in 2010, with 37 % from wastewater treatment, 36 % from the livestock industry, 10 % from biogenic emission, and 9 % from agricultural activity (TEPA 2015). In addition, high amounts of ammonia are released from animal husbandry operations, and fertilizer applications could be sources for the formation of ammonium nitrate (Heo et al. 2013). Elevated NH_3 levels occurred around mid-day, and the NH_4^+ and SO_4^{2-} also increased considerably, indicating that NH_3 likely influenced aerosol particle mass in the summer in Houston. Point sources (e.g., a coal combustion power plant and a chemical plant) might be contributors of NH_3 under favorable meteorological conditions such as high lighting in summertime (Gong et al. 2013).

The fertilizer industry, agricultural fermentation, and farm animal waste could be sources of NH_3 (Walker et al. 2004; Plessow et al. 2005), which may easily transfer into the particulate phase as NH_4^+ through reaction in the atmosphere (Walker et al. 2004; Plessow et al. 2005). High ammonia concentration was determined in the area, especially in winter, and it could neutralize acid gases (such as HNO_3, H_2SO_4, and HCl) to form particles such as NH_4NO_3, $(NH_4)_2SO_4$, and NH_4Cl in particulate matter. NO_3^-, SO_4^{2-}, and NH_4^+ were the dominant ionic composition in the fine particles. NH_4^+ could neutralize SO_4^{2-} and NO_3^- to form $(NH_4)_2SO_4$ and NH_4NO_3, respectively.

In India, high PM concentrations, water-soluble ionic species in PM and precursor gases were determined in the Ganga basin (Behera and Sharma 2010). High NH_3 could come from livestock, open drains, waste collection and disposal conditions, fertilizer application, and biomass burning (Behera and Sharma 2010; Simon et al. 2016). At the Guangdong area in mainland China, high nitric acid and sulfur oxide is associated with the high nitrate and sulfate in PM (Hu et al. 2008). At Shanghai city (Shi et al. 2014), the HNO_3 concentration was similar to that in central Taiwan, but NH_3 concentration was lower than that in central Taiwan (Table 3). In southern Taiwan, high ammonia was observed in the gas precursors in winter. Low temperature and low relative humidity were observed to present a relatively stable condition, and the excess ammonia could transfer into aerosol to form NH_4NO_3 in PM (Tsai et al. 2014).

Concentrations of HCl and SO_2 were higher in the daytime. The concentrations of HNO_3 during the day were about four and five times higher than those at night for Xitun and Jhushan, respectively. The reaction of $NaCl_{(s)}$ and $HNO_{3(g)}$ may have produced HCl near the coastal area (Seinfeld and Pandis 2006). Hence, this reaction cannot completely explain the higher HNO_3 concentration that occurred during the day. NO_2 reacts with hydroxyl radicals during the day and produces HNO_3, which could be another dominant mechanism after sunrise (Russell et al. 1984, 1985). In contrast to HNO_3, the concentrations of HNO_2 and NH_3 at night were about twice as high as those during the day. But high HONO at night could come from source emissions, i.e., combustion engines, especially in diesel-powered vehicles (Kurtenbach et al. 2001) or heterogeneous NO_2–HONO chemical conversion (Su et al. 2008; An et al. 2009; Yu et al. 2009) In addition, nitrous acid was rapidly photolyzed at wavelengths ≤ 400 nm during the day (Calvert et al. 1994). Thus, HNO_2 accumulated mostly at night and was photolyzed by "OH push" after sunrise (Platt and Perner 1980; Acker et al. 2005).

Generally, the retention time of NH_3 may be a few hours in the lower atmosphere, but it could be weeks in a calm environment (Asman and van Jaarsveld 1992). Although a relatively small amount of NH_3 is emitted from industrial processes, the higher NH_3 concentration at night in this study may still be closely related to industrial activities near the sampling sites. Another reason for higher NH_3 may be the stable atmosphere at night (Cadle et al. 1982).

Table 4 shows the meteorological parameters in summer and winter for both stations. At Xitun, the temperature was 26 ± 5 °C during the day and 23 ± 5 °C at night in summer and 25 ± 2 °C during the day and 22 ± 1 °C at night in winter. In addition, the temperature for day/night was 28 ± 2/24 ± 2 °C in summer and 25 ± 2/21 ± 1 °C in winter at Jhushan. The humidity was about 10 % lower during the day than at night for both stations. In addition, the humidity was higher in summer than in winter.

The temperature difference was insignificant ($p > 0.05$) during summer and winter in the area. High wind speeds were determined in the daytime for both stations. Low wind speeds were determined at night, especially in the Jhushan station. The stagnant air flow could cause high PM mass concentration at night (shown as Table 1 and Fig. 3).

The stagnant meteorological conditions could enhance the formation of new secondary species and the long-range transport contributions of pollutants from anthropogenic sources around other air basins associated with high PM concentrations, which was similar to the results of Beijing (Gao et al. 2015).

Based on the back trajectory analysis [developed by Chang's groups (Lin and Chang 2002; Fig. 1)]—the back trajectory was a grid cell model (2 × 2 km)—the air mass was transported over the land to carry the upwind polluted air past the station in the winter. The northerly prevailing monsoon wind affected the wind direction in winter. In summer, the effects of the southerly prevailing monsoon wind

Table 4 Meteorological parameters include temperature, relative humidity, wind speed, and light intensity

Parameter	Xitun				Jhushan			
	Summer		Winter		Summer		Winter	
	Day	Night	Day	Night	Day	Night	Day	Night
T (°C)	25.6 ± 5.4	22.7 ± 5.1	25.3 ± 1.8	21.6 ± 1.4	28.3 ± 2.4	24.3 ± 1.6	25.0 ± 1.5	20.9 ± 0.8
RH (%)	72.2 ± 10.8	86.8 ± 5.1	61.0 ± 4.1	77.3 ± 3.2	68.7 ± 10.3	85.0 ± 5.2	60.9 ± 3.1	76.9 ± 2.2
WS (m s^{-1})	1.8 ± 0.6	1.2 ± 0.4	1.3 ± 0.1	1.1 ± 0.5	1.5 ± 0.3	0.5 ± 0.1	1.1 ± 0.2	0.5 ± 0.1
Global solar radiation (MJ m^{-2})	15.0 ± 3.1		10.7 ± 1.6		12.4 ± 1.7		9.6 ± 0.8	
Duration of sunshine (h)	4.4 ± 1.2		4.4 ± 0.8		3.7 ± 0.9		3.9 ± 0.7	

were insignificant in central Taiwan, although some studies indicated that the air mass moved from south to north and moved inland to Nantou County (Tseng et al. 2009; Simon et al. 2016). The wind rose diagram also reflected this phenomenon (Fig. 3). The land–sea breeze affects the daily fluctuation of wind direction, especially in Jhushan. In addition, some studies have suggested that the mountain-valley wind could be due to the mountains in the vicinity of Jhushan, where the altitude climbs from 100–2,300 m within a distance of less than 10 km (Jhushan township office 2016). Therefore, the topography and solar radiation could affect the transport of air pollutants in the Jhushan area.

Conversion ratio of sulfur and nitrogen species

The nitrogen species conversion ratio is determined as follows (Khoder 2002):

$$F_n = \frac{\left[NO_3^-\right]_p + \left[NO_3^-\right]_g}{\left[NO_2\right]_g + \left[NO_3^-\right]_p + \left[NO_3^-\right]_g} \quad (1)$$

where F_n is the conversion ratio for nitrogen at PM, $[NO_3^-]_p$ is the nitrate concentration in particulate matter, $[NO_3^-]_g$ is the nitric acid concentration in the gas phase, and $[NO_2]_g$ represents the NO_2 concentration in the gas phase.

In winter, the nitrogen conversion ratio was high at both stations during the day and at night. In summer, the average nitrogen conversion ratio was 0.16/0.18 and 0.08/0.09 for day and night, respectively (shown as Table 5). The nitrogen species conversion factor was higher in winter, indicating that lower temperature and relative humidity promoted more rapid formation of NO_3^- and reduced the deliquescence in PM.

The high abundance of pollutants and low wind speed at night cause high nitrogen concentrations at night. In addition, the heterogeneous reaction that produced HNO_3 is important in a nighttime atmosphere with high relative humidity and wet aerosol surface, particularly in winter (Foltescu et al. 1996), which suggests that the hydrolysis of N_2O_5 could be an important source of nitric acid that could cause the nitrogen conversion. The formation of NO_3^- aerosol would be ammonia sensitive (i.e., deficit ammonia), as evidenced by smaller total ammonia concentration than the sum of the total sulfate and nitrate concentrations (Shon et al. 2012).

The sulfur species conversion ratio is determined as follows (Khoder 2002):

$$F_s = \frac{\left[SO_4^{2-}\right]_p}{\left[SO_4^{2-}\right]_p + \left[SO_2\right]_g} \quad (2)$$

where F_s is the conversion ratio for sulfur at PM, $[SO_4^{2-}]_p$ is the sulfate concentration (in microgram per cubic meter) at PM, and $[SO_2]_g$ is the SO_2 concentration (in microgram per cubic meter) in gas phase.

The conversion factor was high at night, especially on episode days. The sulfur conversion ratio was 0.30–0.41 for daytime and 0.41–0.52 for nighttime in summer. Generally, the conversion factor of sulfur species in summer was higher than that in winter, and high conversion ratios were determined at night. Gas-phase oxidation of SO_2 played an important role in the formation of SO_4^{2-} in PM (Gao et al. 2011). Wet aerosol surfaces or droplet-containing aerosols could absorb SO_2, leading to SO_2 oxidation by ozone in droplets, which could be an important mechanism of sulfur conversion. Metals rich in fine particulate matter could enhance the heterogeneous catalytic conversion of SO_2 gas into sulfate in the atmosphere (Clements et al. 2013).

Secondary water-soluble ions are the dominant ions in fine particles at all sampling sites. Homogenous gas-phase formation of nitrate is evidence of the ammonium-rich conditions. In contrast, when the environmental NH_4^+ is poor, SO_4^{2-} and NO_3^- are formed mainly through the heterogeneous reaction of precursor gases with marine and crustal particles, especially in the coarse mode. The sulfur oxidation ratio (SOR) and the nitrogen oxidation ratio (NOR) indicate a high photochemical oxidation property over the entire region (Li et al. 2013). Homogenous gas-phase formation of nitrate is evidenced in the ammonium-rich samples.

Table 5 Gas conversion factors of Fn, Fs, NOR, and NOS in summer and winter

Gas species	Xitun				Jhushan			
	Summer		Winter		Summer		Winter	
	Day	Night	Day	Night	Day	Night	Day	Night
Fn	0.16 ± 0.07[a]	0.09 ± 0.06	0.23 ± 0.06	0.30 ± 0.08	0.18 ± 0.07	0.08 ± 0.09	0.44 ± 0.11	0.19 ± 0.06
Fs	0.36 ± 0.17	0.41 ± 0.16	0.23 ± 0.09	0.49 ± 0.10	0.41 ± 0.14	0.52 ± 0.14	0.25 ± 0.07	0.28 ± 0.07
NOR	0.08 ± 0.05	0.07 ± 0.06	0.14 ± 0.05	0.28 ± 0.09	0.08 ± 0.06	0.07 ± 0.08	0.39 ± 0.11	0.17 ± 0.07
SOR	0.36 ± 0.17	0.41 ± 0.16	0.23 ± 0.09	0.49 ± 0.10	0.41 ± 0.14	0.52 ± 0.14	0.25 ± 0.07	0.28 ± 0.07

$NOR = [NO_3^-]_p/\{[NO_3^-]_p + [NO_2]_g\}$; $SOR = [SO_4^{-2}]_p/\{[SO_4^{-2}]_p + [SO_2]_g\}$

[a] Mean ± standard deviation

In addition, NH_4^+ played an important role in the formation of SO_4^{2-} and NO_3^- in fine particulate matter. However, heterogeneous reaction is the main formation mechanism of SO_4^{2-} and NO_3^-, which tended to be enriched in the coarse mode.

High conversion factor was determined in Jhushan, which could indicate a high fraction of gas precursors (such as SO_2 and NO_2) converted into PM and reflected in the PM concentration at Jhushan, especially in winter.

Conclusions

The fine particulate matter fraction was 0.55–0.59 and 0.61–0.71 of PM_{10} for daytime and nighttime at both stations. There was an insignificant difference of fine particulate matter fraction between seasons. However, high fine particulate fraction was determined at nighttime. Ionic species content ranged from 38 to 53 % for $PM_{2.5}$ and from 43 to 48 % for PM_{10}. Mg^{2+} and Ca^{2+} contributed a large fraction of the total water-soluble ions in coarse particles. But the secondary water-soluble ions (SO_4^{2-}, NO_3^-, and NH_4^+) composed more than 50 % of the total ions and were mainly found in fine particles.

The nitrogen species conversion factor was higher in winter, but that of sulfur was higher in summer. As a result, the formation of SO_4^{2-} and NO_3^- is governed by different conditions in different seasons. Generally, ammonium sulfate is more stable than ammonium nitrate. In winter, the high HNO_3 and NH_3 concentrations and rich ammonium condition ($[NH_4^+]/[SO_4^{2-}] > 2$) could enhance the NH_4NO_3 formation in fine particulate matter. Results indicated that lower temperature and relative humidity promoted NO_3^- formation and reduced the deliquescence in PM. Furthermore, pollutants may be transported from other air basins (Taichung, Changhua, and Yunlin) during the daytime under sea breeze conditions and accumulate at night, resulting in chemical reactions that could account for the high PM concentration at Jhushan and exhibit a PM concentration similar to that at Xitun.

The study integrated the water-soluble ionic species in particulate constituents, gaseous precursors, and meteorological parameters and explained their relationships in summer and winter at both stations. It could be useful to explain the high mass fraction of water-soluble ionic species in PM. However, there is still more than 50 % PM mass constituents not identified (such as organic and elemental compositions) in this work, which could be a limitation for PM composition analysis and determine the formation mechanisms and source contributions of atmospheric PM.

Acknowledgements The authors express their sincere thanks to the National Science Council, Taiwan (NSC-96-2221-E-039-012), for the support.

References

Acker K, Möller D, Auel R, Wieprecht W, Kala D (2005) Concentration of nitrous acid, nitric acid, nitrite and nitrate in the gas and aerosol phase at a site in the emission zone during ESCOMPTE 2001 experiment. Atmos Res 74(1-4):507–524

Aikawa M, Hiraki T, Tomoyose N, Ohizumi T, Noguchi I, Murano K, Mukai H (2013) Local emission of primary air pollutants and its contribution to wet deposition and concentrations of aerosols and gases in ambient air in Japan. Atmos Environ 79:317–323

An J, Zhang W, Qu Y (2009) Impacts of a strong cold front on concentrations of HONO, HCHO, O_3 and NO_2 in the heavy traffic urban area of Beijing. Atmos Environ 43:3454–3459

An J, Wang H, Shen L, Zhu B, Zou J, Gao J, Kang H (2015) Characteristics of new particle formation events in Nanjing, China: effect of water-soluble ions. Atmos Environ 108:32–40

Aneja VP, Wang B, Tong DQ, Kimball H, Steger J (2006) Characterization of major chemical components of fine particulate matter in north Carolina. J Air Waste Manage Assoc 56:1099–1107

Asman WAH, van Jaarsveld JA (1992) A variable-resolution transport model applied for NHx in European. Atmos Environ 26A(3):445–464

Baek BH, Aneja VP, Tong Q (2004) Chemical coupling between ammonia, acid gases, and fine particles. Environ Pollut 129:89–98

Behera SN, Sharma M (2010) Investigating the potential role of ammonia in ion chemistry of fine particulate matter formation for an urban environment. Sci Total Environ 408:3569–3575

Benedict KB, Day D, Schwandner FM, Kreidenweis SM, Schichtel B, Malm WC, CollettJr JL (2013) Observations of atmospheric reactive nitrogen species in Rocky Mountain National Park and across northern Colorado. Atmos Environ 64:66–76

Breysse PN, Delfino RJ, Dominici F, Elder ACP, Frampton MW, Froines JR, Geyh AS, Godleski JJ, Gold DR, Hopke PK, Koutrakis P, Li N, Oberdörster G, Pinkerton KE, Samet JM, Utell MJ, Wexler AS (2013) US EPA particulate matter research centers: summary of research results for 2005–2011. Air Qual Atmos Health 6:333–355

Cadle SH, Countess RJ, Kelley NA (1982) Nitric acid and ammonia in urban and rural locations. Atmos Environ 16:2501–2506

Calvert JG, Stockwell WR (1983) Acid generation in the troposphere by gas-phase chemistry. Environ Sci Technol 17:428–443

Calvert JG, Yarwood G, Dunker A (1994) An evaluation of the mechanism of nitrous acid formation in the urban atmosphere. Res Chem Intermediates 20:463–502

Cao J, Xu H, Xu Q, Chen B, Kan H (2012) Fine particulate matter constituents and cardiopulmonary mortality in a heavily polluted Chinese city. Environ Health Perspect 120:373–378

Clements AL, Buzcu-Guven B, Fraser MP, Kulkarni P, Chellam S (2013) Role of particulate metals in heterogeneous secondary sulfate formation. Atmos Environ 75:233–240

Cohen AJ, Anderson HR, Ostro B, Pandey KD, Krzyzanowski M, Künzli N, Gutschmidt K, Pope A, Romieu I, Samet JM, Smith K (2005) The global burden of disease due to outdoor air pollution. J Toxicol Environ Health A 68:1301–1307

Conti S, Lafranconi A, Zanobetti A, Fornari C, Madotto F, Schwartz J, Cesana G (2015) Cardio respiratory treatments as modifiers of the relationship between particulate matter and health: a case-only analysis on hospitalized patients in Italy. Environ Res 136:491–499

Foltescu VL, Selin Lindgern E, Isakson J, Öblad M, Pacyna JM, Benson S (1996) Gas-to-particle conversion of sulfur and nitrogen compounds as studied at marine stations in northern European. Atmos Environ 30:3129–3140

Gao X, Yang L, Cheng S, Gao R, Zhou Y, Xue L, Shou Y, Wang J, Wang X, Nie W, Xu P, Wang W (2011) Semi-continuous measurement of water-soluble ions in PM2.5 in Jinan, China: temporal variations and source apportionments. Atmos Environ 45:6048–6056

Gao J, Tian H, Cheng K, Lu L, Zheng M, Wang S, Hao J, Wang K, Hua S, Zhu C, Wang Y (2015) The variation of chemical characteristics of $PM_{2.5}$ and PM_{10} and formation causes during two haze pollution events in urban Beijing, China. Atmos Environ 107:1–8

Gauvin S, Reungoat P, Cassadou S, DéchenauxMomas I, Just J, Zmirou D (2002) Contribution of indoor and outdoor environments to $PM_{2.5}$ personal exposure of children-VESTA study. Sci Total Environ 297(1-3):175–181

Glodberg MS, Burnett RT, Bailar JC III, Brook J, Bonvalot Y, Tamblyn R, Singh R, Valois M, Vincent R (2001) The association between daily mortality and ambient air particle pollution in Montreal Quebec 2. Cause-specific mortality. Environ Res A 86(1):26–36

Gong L, Lewicki R, Griffin RJ, Tittel FK, Lonsdale CR, Stevens RG, Pierce JR, Malloy QGJ, Travis SA, Bobmanuel LM, Lefer BL, Flynn JH (2013) Role of atmospheric ammonia in particulate matter formation in Houston during summertime. Atmos Environ 77:893–900

Han YJ, Kim TS, Kim H (2008) Ionic constituents and source analysis of $PM_{2.5}$ in three Korea cities. Atmos Environ 42:3127–3141

Harrison RM, Kito AMN (1990) Field intercomparison of filter pack and denuder sampling methods for reactive gaseous and particulate pollutants. Atmos Environ 24:2633–2640

Harrison RM, Pio CA (1983) Size-differentiated composition of inorganic atmospheric aerosols of both marine and continental origin. Atmos Environ 17:1733–1738

Heald CL, Collett JL, Lee T, Benedict KB, Schwandner FM, Li Y, Clarisse L, Hurtmans DR, Damme MV, Clerbaux C, Coheur PF, Pye HOT (2012) Atmospheric ammonia and particulate inorganic nitrogen over the United States. Atmos Chem Phys 12:10295–10312

Heitzenberg J (1989) Fine particles in the global troposphere: a review. Tellus 41B:149–160

Heo J, McGinnis JE, de Foy B, Schauer JJ (2013) Identification of potential source areas for evaluated $PM_{2.5}$, nitrate and sulfate concentrations. Atmos Environ 71:187–197

Hitchcock DR, Spiller LL, Wilson WE (1980) Sulfuric acid aerosols and HCl release in coastal atmospheres: evidence of rapid formation of sulfuric acid particulates. Atmos Environ 14:165–182

Hoek G, Meliefste K, Cyrys J, LewnéBellander T, Brauer M, Fischer P, Gehring U, Heinrich J, van Vliet P, Brunekreef B (2002) Spatialvariabilityoffineparticleconcentrations in three European areas. Atmos Environ 36(25):4077–4088

Horemans B, Krata A, Buczynska AJ, Dirtu AC, Van Meel K, Van Grieken R, Bencs L (2009) Major ionic species in size-segregated aerosols and associated gaseous pollutants at a coastal site on the Belgian North Sea. J Environ Monit 11:670–677

Hsieh LY, Kuo SC, Chen CL, Tsai YI (2009) Size distribution of nano/micro dicarboxylic acids and inorganic ions in suburban PM episode and non-episodic aerosol. Atmos Environ 43:4396–4406

Hu JH, Abbatt JPD (1997) Reaction probabilities for N_2O_5 hydrolysis on sulfuric acid and ammonium sulfate aerosols at room temperature. J Phys Chem A 101:871–878

Hu M, Wu Z, Slanina J, Lin P, Liu S, Zeng L (2008) Acidic gases, ammonia and water-soluble ions in $PM_{2.5}$ at a coastal site in the Pearl River Delta, China. Atmos Environ 42:6310–6320

Jalaludin BB, O'Toole BI, Leeder SR (2004) Acute effects of urban ambient air pollution on respiratory symptoms, asthma medication use, and doctor visits for asthma on a cohort of Australian children. Environ Res 95(1):32–42

Jhushan township office (2016) http://www.chushang.gov.tw, (accessed at March, 2016).

Kadowaki S (1977) Size distribution and chemical composition of atmospheric particulate nitrate in the Nagoya area. Atmos Environ 11:671–675

Kang S, Mayewski PA, Qin D, Sneed SA, Ren J, Zhang D (2004) Seasonal differences in snow chemistry from the vicinity of Mt. Everest, central Himalayas. Atmos Environ 38:2819–2829

Kappos AD, Bruckmann P, Eikmann T, Englert N, Heinrich U, Höppe P, Koch E, Krause GHM, Kreyling WG, Rauchfuss K, Rombout P, Schulz-Klemp V, Thiel WR, Wichmann HE (2004) Health effects of particles in ambient air. Int J Hyg Environ Health 207(4):399–407

Khoder MI (2002) Atmospheric conversion of sulfur dioxide to particulate sulfate and nitrogen dioxide to particulate nitrate and gaseous nitric acid in an urban area. Chemosphere 49:675–684

Kim KH, Kabir E, Kabir S (2015) A review on the human health impact of airborne particulate matter. Environ Int 74:136–143

Kirkby J, Curtius J, Almeida J, Dunne E, Ehrhart S, Duplissy J et al (2011) Role of sulfuric acid, ammonia and galactic cosmic rays in atmospheric aerosol nucleation. Nature 476:429–433

Kurtenbach R, Becker KH, Gomes JAG, Kleffmann J, Lörzer JC, Spittler M, Wiesen P, Ackermann R, Geyer A, Platt U (2001) Investigations of emissions and heterogeneous formation of HONO in a road traffic tunnel. Atmos Environ 35:3385–3394

Li X, Wang L, Ji D, Wen T, Pan Y, Sun Y, Wang Y (2013) Characterization of the size-segregated water-soluble inorganic ions in the Jing-Jin-Ji urban agglomeration: Spatial/temporal variability, size distribution and sources. Atmos Environ 77:250–259

Li Y, Schwandner FM, Sewell HJ, Zivkovich A, Tigges M, Raja S, Holcomb S, Molenar JV, Sherman L, Archuleta C, Lee T, Collett JL Jr (2014) Observations of ammonia, nitric acid, and fine particles in a rural gas production region. Atmos Environ 83:80–89

Lin JJ (2002) Characterization of the major chemical species in $PM_{2.5}$ in the Kaohsiung city, Taiwan. Atmos Environ 36:1911–1920

Lin CH, Chang LFW (2002) Relative source contribution analysis using an air trajectory statistical approach. J Geophys Res 107(D21):4583. doi:10.1029/2001JD001301

Lin YC, Cheng MT, Ting WY, Yeh CR (2006) Characteristics of gaseous HNO2, HNO3, NH3 and particulate ammonium nitrate in an urban city of central Taiwan. Atmos Environ 40:4725–4733

Lin CC, Huang KL, Chen SJ, Liu SC, Tsai JH, Lin YC, Lin WY (2009) NH_4^+, NO_3^- and SO_4^{2-} in roadside and rural size-resolved particles and transformation of NO_2/SO_2 to nanoparticle-bound NO_3^- / SO_4^{2-}. Atmos Environ 43:2731–2736

Minguillón MC, Querol X, Baltensperger U, Prévôt ASH (2012) Fine and coarse PM composition and sources in rural and urban sites in Switzerland: local or regional pollution? Sci Total Environ 427–428:191–202

Ocskay R, Salma I, Wang W, Maenhaut W (2006) Characterization and diurnal variation of size-resolved inorganic water-soluble ions at a rural background site. J Environ Monit 8:300–306

Okada K, Ikegami M, Zaizen Y, Makino Y, Jensen JB, Gras JL (2001) The mixture state of individual aerosol particles in the 1997 Indonesian haze episode. J Aerosol Sci 32:1269–1279

Pathak RK, Wang T, Wu WS (2011) Nighttime enhancement of $PM_{2.5}$ nitrate in ammonia-poor atmospheric conditions in Beijing and Shanghai: plausible contributions of heterogeneous hydrolysis of N_2O_5 and HNO_3 partitioning. Atmos Environ 45:1183–1191

Perrino C, DeSantis F, Febo A (1990) Criteria for the choice of a denuder sampling technique devoted to the measurement of atmospheric nitrous and nitric acids. Atmos Environ 24A:617–626

Phan NT, Kim KH, Shon ZH, Jeon EC, Jung K, Kim NJ (2013) Analysis of ammonia variation in the urban atmosphere. Atmos Environ 65: 177–185

Pio CA, Lopes DA (1998) Chlorine loss from marine aerosol in a coastal atmosphere. J Geophys Res 103:25263–25272

Platt U, Perner D (1980) Direct measurements of atmospheric CH_2O, HNO_2, O_3, NO_2 and SO_2 by differential optical absorption in the near UV. J Geophs Res 85(C12):7453–7458

Plaza J, Pujadas M, Gómez-Moreno FJ, Sánchez M, Artíñano B (2011) Mass size distribution of soluble sulfate, nitrate and ammonium in the Madrid urban aerosol. Atmos Environ 45:4966–4976

Plessow K, Spindler G, Zimmermann F, Matschullat J (2005) Seasonal variations and interactions of N-containing gases and particles over a coniferous forest, Saxony, Germany. Atmos Environ 39(37):6995–7007

Ravishankara A (1997) Heterogeneous and multiphase chemistry in the troposphere. Science 276:1058–1065

Reche C, Viana M, Pandolfi M, Alastuey A, Moreno T, Amato F, Ripoll A, Querol X (2012) Urban NH_3 levels and sources in a Mediterranean environment. Atmos Environ 57:153–164

Russell AG, McRae GJ, Cass GR (1984) Acid deposition of photochemical oxidation products-a study using a Lagrangian trajectory models. In: De Wispelaere C (ed) Air pollution modeling and its application III. Plenem press, New York, pp 539–564

Russell AG, McRae GJ, Cass GR (1985) The dynamics of nitric acid production and the fate of nitrogen oxides. Atmos Environ 19: 893–902

Sakurai T, Fujita S (2002) Analysis of atmospheric ammonia budget for the Kanto region, Japan. Atmos Environ 36:4201–4209

Seinfeld JH, Pandis SN (2006) Atmospheric chemistry and physics: from air pollution to climate change. John Wiley & Sons Inc, New York

Shen J, Liu X, Zhang Y, Fangmeier A, Goulding K, Zhang F (2011) Atmospheric ammonia and particulate ammonium from agricultural sources in the North China Plain. Atmos Environ 45:5033–5041

Shi Y, Chen J, Hu D, Wang L, Yang X, Wang X (2014) Airborne submicron particulate (PM1) pollution in Shanghai, China: Chemical variability, formation/dissociation of associated semi-volatile components and the impacts on visibility. Sci Total Environ 473–474: 199–206

Shon ZH, Kim KH, Song SK, Jung K, Kim NJ, Lee JB (2012) Relationship between water-soluble ions in $PM_{2.5}$ and their precursor gases in Seoul megacity. Atmos Environ 59:540–550

Simon S, Klemm O, El-Madany T, Walk J, Amelung K, Lin PH, Chang SC, Lin NH, Engling G, Hsu SC, Wey TH, Wang YN, Lee YC (2016) Chemical composition of fog water at four sites in Taiwan. Aerosol Air Qual Res 16:618–631

Spengler JD, Brauer M, Koutrakis P (1990) Acid air and health. Environ Sci Technol 24(7):946–955

Su H, Cheng YF, Cheng P, Zhang YH, Dong S, Zeng LM, Wang X, Slanina J, Shao M, Wiedensohler A (2008) Observation of nighttime nitrous acid (HONO) formation at a non-urban site during PRIDE-PRD2004 in China. Atmos Environ 42:6219–6232

Sudheer AK, Rengarajan R (2015) Time-resolved inorganic chemical composition of fine aerosol and associated precursor gases over an urban environment in western India: gas-aerosol equilibrium characteristics. Atmos Environ 109:217–227

Sun YL, Zhuang GS, Tang AH, Wang Y, An ZS (2006) Chemical characteristics of $PM_{2.5}$ and PM_{10} in haze-fog episodes in Beijing. Environ Sci Technol 40:3148–3155

Sun YL, Jiang Q, Wang ZF, Fu PQ, Li J, Yang T, Yin Y (2014) Investigation of the sources and evolution processes of severe haze pollution in Beijing in January 2013. J Geophys Res Atmos 119: 4380–4398

Tan JH, Duan JC, He KB, Ma YL, Duan FK, Chen Y, Fu JM (2009) Chemical characteristics of $PM_{2.5}$ during a typical haze episode in Guangzhou. J Environ Sci 21:774–781

TEPA (Taiwan Environmental Protection Agency) (2015) Air Pollutants Emission Database and Air Quality Management Program. Taipei, Taiwan

Thibert E, Domine' F (1997) Thermodynamics and kinetics of the solid solution of HCl in ice. J Phys Chem B 101:3554–3565

Tsai YI, Chen CL (2006) Atmospheric aerosol composition and source apportionments to aerosol in southern Taiwan. Atmos Environ 40: 4751–4763

Tsai JH, Chang TC, Huang YS, Shieh ZX, Chiang HL (2011) Particulate composition characteristics under different ambient air quality conditions. J Air Waste Manage Assoc 61:796–805

Tsai JH, Chang LP, Chiang HL (2013) Size mass distribution of water-soluble ionic species and gas conversion to sulfate and nitrate in particulate matter in southern Taiwan. Environ Sci Pollut Res 20: 4587–4602

Tsai JH, Chang LP, Chiang HL (2014) Airborne pollutant characteristics in an urban, industrial and agricultural complex metroplex with high emission loading and ammonia concentration. Sci Total Environ 494–495:74–83

Tseng KH, Wang JL, Cheng MT, Tsuang BJ (2009) Assessing the relationship between air mass age and summer ozone episodes based on photochemical indices. Aerosol Air Qual Res 9:149–171

U.S. Environmental Protection Agency (USEPA) (1998) Compendium of methods for the determination of inorganic compounds in ambient air –IO-4.2 determination of reactive acid and basic gases and strong acidity in fine particles. USEPA publication 625/R-96/010a, Cincinnati

Vianaa AM, Pe'rezb C, Querola X, Alastueya A, Nickovicc S, Baldasano JM (2005) Spatial and temporal variability of PM levels and composition in a complex summer atmospheric scenario in Barcelona (NE Spain). Atmos Environ 39:5343–5361

Wakamatsu S, Utsunomiya A, Han JS, Mori A, Uno I, Uehara K (1996) Seasonal variation in atmospheric aerosol concentration covering Northern Kyushu, Japan and Seoul, Korea. Atmos Environ 30: 2343–2354

Walker JT, Whitall DR, Robarge W, Paerl HW (2004) Ambient ammonia and ammonium aerosol across a region of variable ammonia emission density. Atmos Environ 38(9-10):1235–1246

Wall SM, John W, Ondo JL (1988) Measurement of aerosol size distributions for nitrate and major ionic species. Atmos Environ 22:1649–1656

Wang D, Hu J, Xu Y, Lv D, Xie X, Kleeman M, Xing J, Zhang H, Ying Q (2014) Source contributions to primary and secondary inorganic particulate matter during a severe wintertime $PM_{2.5}$ pollution episode in Xi'an, China. Atmos Environ 97:182–194

Ying Q, Kleeman MJ (2006) Source contributions to the regional distribution of secondary particulate matter in California. Atmos Environ 40:736–752

Yu Y, Galle B, Panday A, Hodson E, Prinn R, Wang S (2009) Observations of high rates of NO_2-HONO conversion in the nocturnal atmospheric boundary layer in Kathmandu, Nepal. Atmos Chem Phys 9:6401–6415

Zhang B, Tao FM (2010) Direction homogeneous nucleation of NO_2, H_2O and NH_3 for the production of ammonium nitrate particles and HONO gas. Chem Phys Lett 489:143–147

Zhang H, Hu J, Kleeman M, Ying A (2014) Source apportionment of sulfate and nitrate particulate matter in the eastern United States and effectiveness of emission control programs. Sci Total Environ 490: 171–181

Zhu T, Shang J, Zhao D (2011) The roles of heterogeneous chemical processes in the formation of an air pollution complex and gray haze. Sci China Chem 54(1):145–153